

Contribution of charm annihilation to the hyperfine splitting in charmonium in the quenched case

L. Levkova* and **C. DeTar**

University of Utah, Salt Lake City, UT 84112, USA

E-mail: ludmila@phys.columbia.edu, detar@physics.utah.edu

Fermilab Lattice and MILC Collaborations

In calculations of the hyperfine splitting in charmonium, the contributions of the disconnected diagrams is considered small and is typically ignored. We aim to estimate nonperturbatively the size of the resulting error, which could potentially affect the high precision calculations of the charmonium spectrum. Following our work on the effects of the disconnected diagrams in unquenched QCD presented at Lattice 2007, we study the same problem in the quenched case. On dynamical ensembles the disconnected charmonium propagators contain light modes which complicate the extraction of the signal at large distances. In the fully quenched case, where there are no such light modes, the interpretation of the signal is simplified. We present results from lattices with $a \approx 0.09$ fm and $a \approx 0.063$ fm.

The XXVI International Symposium on Lattice Field Theory

July 14 - 19, 2008

Williamsburg, Virginia, USA

*Speaker.

1. Introduction

Lattice calculations of the hyperfine splitting in charmonium usually ignore the contributions of the disconnected diagrams. This simplification leads to an error and our goal is to determine its degree and thus elucidate the origins of the the current discrepancies between the lattice calculations and the experimental value of the hyperfine splitting of 117 MeV. The discrepancy, which even for improved actions [1, 2] is within 10% below the experimental value, could be a result both of the omission of the disconnected diagrams and of the discretization errors in the heavy-quark actions. Our work on dynamical lattices reported in [3], improved over previous attempts [4, 5] to determine the effect of the disconnected diagrams by going to finer lattice spacings, larger volumes, using unbiased subtraction for the stochastic estimation of the operator traces, and most importantly, using point-to-point (*ptp*) propagators. This allowed us to estimate that the contribution of the disconnected diagrams decreases the lattice hyperfine splitting, which implied that the main culprit for the discrepancy between lattice and experiment is the discretization error in the heavy-quark action. Our estimation was based on fits of the disconnected *ptp* propagators to an asymptotic formula which did not take into account the rotational symmetry violations visible in our data. Here we introduce a new procedure which should take these effects into account and we study the effect on quenched lattices, where complications from light-quark intermediate states are absent.

The full charmonium propagator, $F(t)$, is a sum of two contributions, connected, $C(t)$, and disconnected, $D(t)$, shown in Fig. 1:

$$F(t) = C(t) + D(t) = \sum_n \langle 0|O|n\rangle \langle n|O|0\rangle e^{-E_n t}. \quad (1.1)$$

The mass shift due to charm quark loops can be treated as a perturbation, in which case, to first order, both contributions can be computed without charmed sea quarks. The operator O is defined to be hermitian, in which case $F(t) \geq 0$ for all t . This is also true if we consider the *ptp* propagator $F(r)$ instead, where r is the Euclidian distance on the lattice. The matrix defining the spin structure in the operator O is $\Gamma = \gamma_5, \gamma_i$ for the η_c and J/Ψ states, respectively. The parameter λ in the disconnected diagram in Fig. 1 stands effectively for the various interactions that can occur between the two quark loops. Its origins can be a combination of the $U_A(1)$ anomaly effects, glueball interactions and in the dynamical case – the propagation of light hadronic modes. At large distances the light modes, if they exist, should dominate in $F(r)$. Since $F(r)$ is nonnegative for all r , it follows that in this case $D(r)$ should also be nonnegative in the large distance limit. The sign of $D(r=0)$, with the above hermiticity condition on O , is strictly negative for the pseudoscalar (and positive for the vector). It follows that in the dynamical case $D(r)$ changes sign for the pseudoscalar, and indeed we observed this sign flip [3]. In the quenched case this sign flip would occur only if there are glueballs lighter than the charmonium state studied and their signal is stronger than the noise in the data at large distances. A simplified form which describes the behavior of $D(r)$ in momentum space is

$$D(p^2) \sim \underbrace{\left(C + \frac{f}{p^2 + m_l^2} \right)}_{\lambda} \left(\frac{a}{p^2 + m_c^2} + \frac{b}{p^2 + m_c^{*2}} \right)^2, \quad (1.2)$$

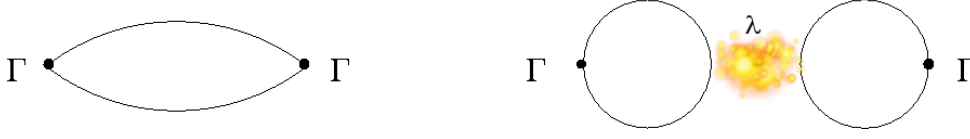


Figure 1: Connected (left) and disconnected (right) diagrams contributing to the full propagator on lattices quenched with respect to the charm quark.

where we have included in the quark loops one ground state, characterized by mass m_c and an excited one with mass m_c^* . The parameter λ is represented by a sum of two terms: C stands for possible effects of the $U_A(1)$ anomaly (or other effects which cannot be decomposed spectrally) and $f/(p^2 + m_l^2)$ is an effective light mode term. If in Eq. (1.2) we use $4 \sin^2(p_\mu a/2)$ in place of $(p_\mu a)^2$, its discrete Fourier transform accounts for violations of rotational symmetry. As in [3] the masses m_c and m_c^* have been determined from fits to the connected charmonium propagators and are kept fixed. Then the mass shift due to the disconnected diagram contribution can be approximated as follows

$$\Delta m = m_c - m_f = \frac{\lambda(-m_c^2)a^2}{\sqrt{32}A_t m_c^2}, \quad (1.3)$$

where m_f is the full propagator mass and the amplitude A_t is determined from the timeslice-to-timeslice connected diagram charmonium propagator. The sign of the mass shift depends on the sign of $\lambda(-m_c^2)$.

2. Dynamical case

Fitting our results for $D(r)$ in the dynamical case (for details see [3]) directly to Eq. (1.2) does not work – our model most probably has too many parameters and requires higher quality statistics. We are forced to make further simplifications in our fitting form by removing the light modes from the data. We subtracted the asymptotic form $Le^{-m_l r}/r^{\frac{3}{2}}$ with values of the parameters L and m_l which we already determined in [3]. The data for $D_{\eta_c}(r)$ before and after the subtraction is shown in Fig. 2. We fit the subtracted data to the form below, where in this case the absolute value of C is absorbed in the parameters a and b and only its sign remains:

$$D(p^2) \sim \text{sign}(C) \left(\frac{a}{p^2 + m_c^2} + \frac{b}{p^2 + m_c^{*2}} \right)^2. \quad (2.1)$$

The masses m_c and m_c^* are the same values used in the fits in [3]. Using the above form allows us to obtain a good χ^2/DoF , but the fits do not deliver consistent results when we change the fitting range or consider just one ground state. Fig. 2, where we show two fits with $\chi^2/\text{DoF} \approx 1$, illustrates the problem. The first fit (green) is a two state fit as in Eq. (2.1) and yields $\Delta m_{\eta_c} = -0.7(5)$ MeV. The second fit (blue) is a ground state fit only, with the range of r shifted to larger values. This fit gives $\Delta m_{\eta_c} = -5.5(4)$ MeV. These two values, although consistent with our rough estimates from [3], are not consistent with each other within the errors obtained from the fits, suggesting a substantial systematic error. We also have results for $D_{J/\psi}(r)$, shown in Fig. 3. The signal for the vector is much more noisy and falls off into the noise at much shorter distances than it does in the

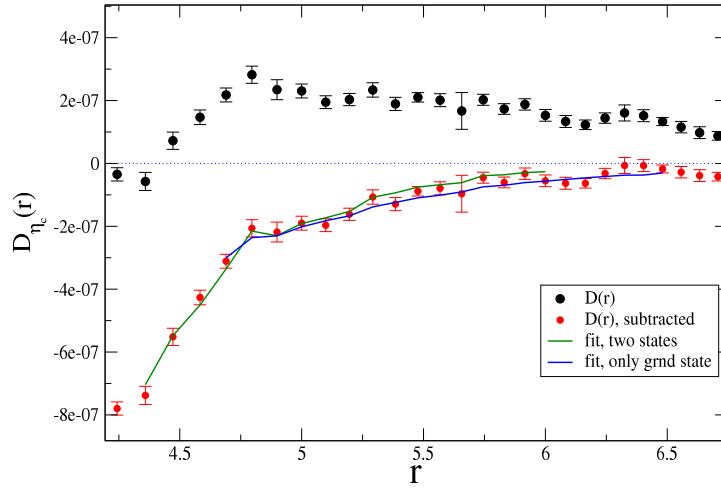


Figure 2: The disconnected ptp propagator for η_c in the dynamical case before and after the subtraction of the light modes. Also shown are fits to the data after subtraction with one and two states.

pseudoscalar case (due to the larger mass of the J/Ψ). We can make only rough estimations for the values of the disconnected diagram in this case: $-1 \text{ MeV} < \Delta m_{J/\Psi} < 0 \text{ MeV}$. These results show

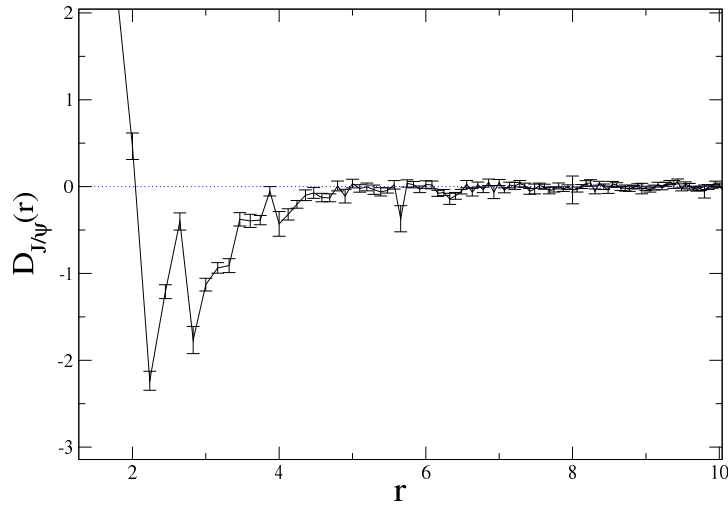


Figure 3: The disconnected ptp propagator for J/Ψ in the dynamical case.

that the dynamical case requires a better understanding and further study.

3. Quenched case

In the quenched case the behavior of the disconnected propagator is expected to be simplified due to the absence of light hadronic modes propagating at large distances. As in [3] we use clover fermions to represent the charm quarks on the lattice. We have results for two quenched ensembles, “fine” and “superfine”, with lattice spacing of $a \approx 0.09 \text{ fm}$ and 0.063 fm , respectively. The lattice

volume for the fine ensemble is $28^3 \times 96$ and for the superfine it is $48^3 \times 144$. The respective sizes of the ensembles are 366 and 124 configurations, and the charm quark kappas are $\kappa = 0.127$ and 0.130. It is interesting to compare $D_{\eta_c}(r)$ on the fine quenched ensemble with the dynamical result at the same lattice spacing of $a \approx 0.09$ fm. Figure 4 shows that the main difference is that the sign of $D_{\eta_c}(r)$ stays constant in the region where we see the dynamical data flip sign. We interpret the behavior of the quenched data as evidence that in the region where we have a clear signal, not only are there no light meson modes due to the quenching, but also if there are glueballs lighter than the η_c in our case at all, their signal is very weak. This makes the use of the fitting form of Eq. (2.1) justifiable in this case. The fits in the quenched case give consistent results under changes

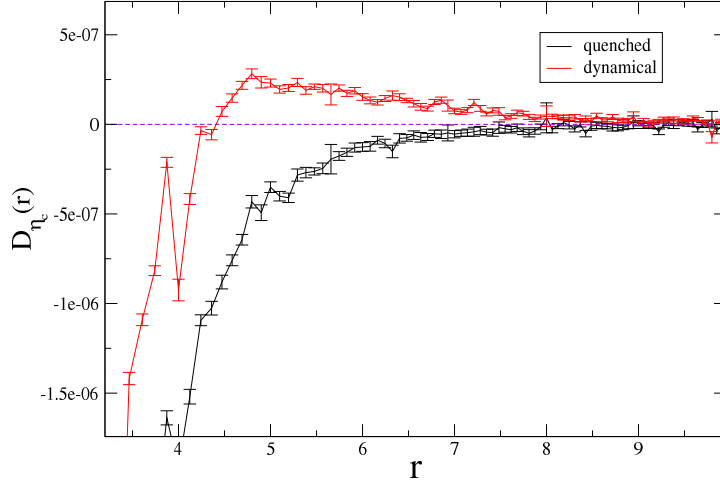


Figure 4: Comparison between the η_c dynamical and quenched disconnected propagators at the same lattice spacing of $a \approx 0.09$ fm.

of the fit range and number of states. The result for $D_{\eta_c}(r)$ on the fine ensemble is shown in Fig. 5. The fit to $D_{\eta_c}(r)$ is done with $m_c = 0.9781$, $m_c^* = 1.330$, known with high accuracy from fits to the connected propagator. The fitting range is $r = 4.3 - 7.8$ and the fit has $\chi^2/\text{DoF} = 40/40$. We obtain $a = 109(15)$ and $b = 294(41)$ for the fit parameters in Eq. (2.1). This yields $\Delta m_{\eta_c} = -3.3(9)\text{MeV}$.

We treat the superfine ensemble results similarly. They are shown in Fig. 6. From the fit which is done with $m_c = 0.6509$, $m_c^* = 0.8606$ and fitting range $r = 5.6 - 8$ with $\chi^2/\text{DoF} = 31/31$, we obtain $a = 131(17)$ and $b = 246(38)$. This means $\Delta m_{\eta_c} = -3.1(8)\text{MeV}$ from the superfine calculation. The results from both quenched fine and superfine calculations are consistent with each other and with the rough estimates from the dynamical case. They show that the η_c mass is slightly increased due to the disconnected diagram contribution. We also studied the disconnected propagator for J/Ψ in the quenched case. Figure 7 shows $D_{J/\Psi}(r)$ on both fine and superfine lattices. The behavior of the data in both cases is similar: the noise is larger than it is in the pseudoscalar case, and the signal for the state is overwhelmed by the noise at shorter r . Fits to the data have good χ^2/DoF but the error on the fit parameters are very large. At this point we can only estimate that, similarly to the dynamical case, $-1 \text{ MeV} < \Delta m_{J/\Psi} < 0 \text{ MeV}$.

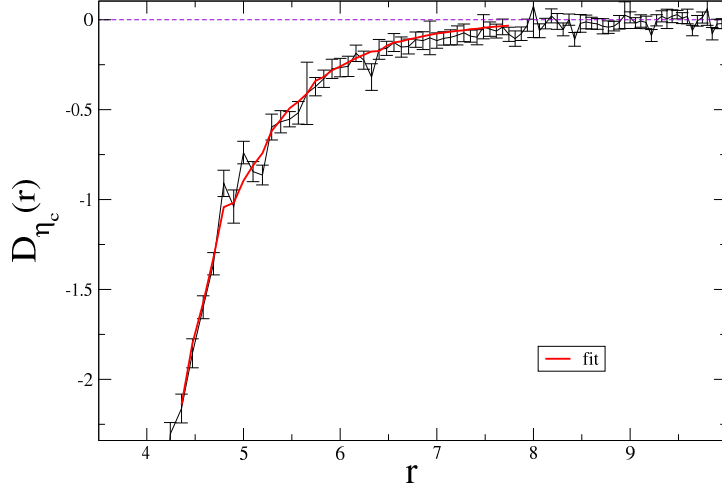


Figure 5: The disconnected ptp propagator for η_c on the fine quenched lattices ($a \approx 0.09$ fm).

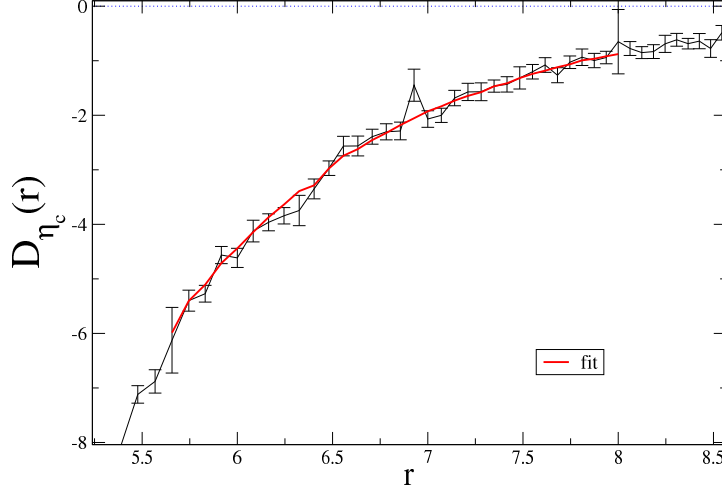


Figure 6: The disconnected ptp propagator for η_c on the superfine quenched lattices ($a \approx 0.063$ fm).

4. Conclusions

We studied the contributions of the disconnected diagrams to the masses of η_c and J/Ψ in the dynamical and the simplified quenched cases. We introduced a new fitting procedure which takes into account rotational symmetry violations. It gives consistent results with our previous fitting method, but the dynamical case requires further study to make more accurate predictions. The quenched results for Δm_{η_c} are the same within error for two lattice spacings 0.09 and 0.063 fm: $-3.3(9)$ and $-3.1(8)$ MeV, respectively. This consistency suggests that the discretization errors are smaller than our statistical errors. Our results show that the disconnected diagram contributions increase the η_c mass, which is contrary to the perturbative estimate of a 2.4 MeV decrease [2]. The mechanism of this increase can be a combination of two effects: mixing with glueballs with masses

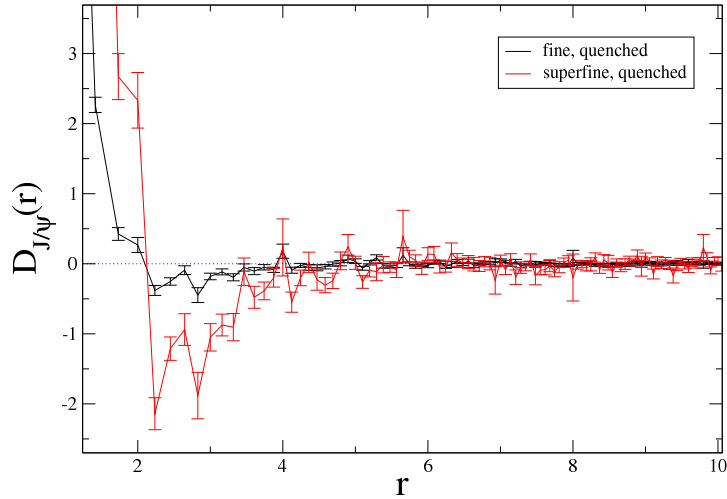


Figure 7: The disconnected ptp propagator for J/Ψ on the fine and superfine quenched lattices.

lower than the mass of the η_c and the influence of the $U_A(1)$ anomaly. In our case the pole mass of the η_c is lighter than the physical one by about 1 GeV. This is due to the fact that the κ -tuning for the charm quark was done for the kinetic mass instead of the pole mass. The lightness of our η_c means that there is no lighter glueball to mix with [6] and the increase of its mass is due to the anomaly alone. We are currently starting a quenched calculation at smaller charm quark kappa, which would give a pole mass closer to the physical one for η_c . We want to rule out the possibility that the mass increase in the η_c we observe is an artifact of the current light pole mass. In the case of the vector state J/Ψ , in both dynamical and quenched cases, we can only estimate that its mass will increase by an amount smaller than 1 MeV as a result of the disconnected diagram contributions. We need higher statistics to be able to achieve a better estimate since the signal in the vector case is noisier and falls off rather quickly with r due to the fact that the vector state is heavier than the pseudoscalar. We conclude that as a whole, the hyperfine splitting will decrease by an amount up to a few MeV when the disconnected diagrams are taken into account in the lattice charmonium calculations. This means that the discrepancies between the lattice calculations (based solely on connected diagrams) and the experiment are more likely attributable to heavy quark discretization errors.

References

- [1] S. Gottlieb *et al.*, PoS(LAT2006) 175.
- [2] E. Follana *et al.*, Phys. Rev. **D75** (2007) 054502 [hep-lat/054502].
- [3] C. DeTar and L. Levkova, PoS(LAT2007) 116, arXiv:0710.1322 [hep-lat].
- [4] C. McNeile and C. Michael, Phys. Rev. **D70** (2004) 034506 [hep-lat/0402012].
- [5] P. de Forcrand *et al.* [QCD-TARO Collaboration], JHEP 0408 (2004) 004 [hep-lat/0404016].
- [6] Y. Chen *et al.*, Phys. Rev. **D73:014516** (2006), [hep-lat/0510074].